J Mater Sci (2007) 42:4191–4196
DOI 10.1007/s10853-006-0641-3

Interfacial stress transfer of fiber pullout for carbon nanotubes with a composite coating

Toshiaki Natsuki · Feng Wang · Q. Q. Ni · Morinobu Endo

Received: 15 January 2006 / Accepted: 5 July 2006 / Published online: 2 March 2007

Abstract An analytical approach has been established to evaluate the interfacial stress transfer characteristics of single- and multi-walled carbon nanotubes (CNTs) with composite coatings by means of fiber pullout model. According to the present model, the effects of several parameters such as coating thickness, layer numbers and dimension of CNTs on interfacial stress transfers were investigated and analyzed. The results suggested that the maximum interfacial shear stress occurred at the pullout end of CNTs and decreased with increasing coating thickness as well as CNT wall thickness (layer numbers). Moreover, the distribution of the interfacial shear and coating axial stress along the CNT length was found to be largely affected by the friction coefficient in the interface between the CNT and the coating layer.

Introduction

Carbon nanotubes (CNTs) possess many unique properties such as high strength and elastic modulus [1–4], and outstanding thermal and electrical conductivities [4, 5]. Significant interest has been recently focused on CNT composites that enhance mechanical and electrical characteristics more than those of the host materials [5–8]. As a creative chemical method for surface modifications, coatings on CNTs have also received much attention and then have been investigated by a large number of researchers [9–13]. Chen and co-workers [8–10] presented an electroless plating method for preparing the Ni–P/CNT composite coatings. They reported that the Ni–P/CNT composite coatings not only possess the higher wear resistance but also show the lower friction coefficient. Seeger el al. [11] described a colloidal method at room temperature for preparation of SiO_x-coating of CNTs using a sol–gel technique. They demonstrated that the coatings prepared through a high-temperature route tend to be more unstable compared with those deposited at room temperature. Han and Zettl [12] have coated thin SnO_2 layers on surfaces of single-walled carbon nanotubes (SWCNTs) through a simple chemical-solution route. They then proposed that the Sn–C bonding possibly formed in the interfaces between SnO_2 layers and nanotubes might change the localized electron system of CNTs. Shi et al. [14, 15] reported a plasma polymerization treatment for preparing the polymer ultrathin films (1~3 nm) on CNTs surface. To assemble nanoscale electronic devices, an insulating layer should be coated onto the CNTs to avoid short circuits, polymer-coated CNTs have been recently used as a scanning tip for atomic force microscopy (AFM) and have shown great potential application for nanoscale bio- and electrochemical probing [16]. In these studies, however, no any analysis has been focused on the interfacial bonding and the stress transfer effective in the interface between the CNTs and the coatings.

Interfacial structures of CNTs with composite coatings are one of the very important factors in the CNT composite applications for determining their

T. Natsuki (✉) · Q. Q. Ni
Faculty of Textile Science & Technology, Shinshu University, 3-15-1 Tokida, Ueda-shi 386-8567, Japan
e-mail: natsuki@endomoribu.shinshu-u.ac.jp

F. Wang · M. Endo
Faculty of Engineering, Shinshu University, Wakasato 4-17-1, Nagano-shi 380-8553, Japan

mechanical behavior as well as thermal and electrical conductivities. The internal stress within the coated CNTs is thought to have a propensity to cause the structural failure, which affects some physical properties of CNT composites. Thus, it is crucial to investigate the interfacial debonding and the stress transfers in the interfaces between the CNTs and the coatings. Typically, the higher fiber aspect ratio is available for an efficient stress transfer between matrix and fibers due to the larger interface area [17].

We face a tremendous challenge for the experimental characterization of CNTs with extremely small dimensions. Accordingly, it is still difficult to conduct the straight measurements of the interfacial stress transfer of single or multi-walled CNTs with coatings although some experimental techniques have been developed to analyze their tensile stress behaviors. The interfacial bonding and the stress transfer in CNT composites are complex; some of the most important factors such as the dimensions of CNTs and the coating thickness would influence the stress transfer efficiency. A few studies [18–20] have been reported on the characterization of the mechanical properties between CNTs and matrix materials. Lau [18] has studied the interfacial bounding characteristics of CNT-polymer composites by a conventional model [21]. Recently, Zhang and Wang [19] have reported the interfacial stress transfer characteristics of CNT-polymer composites under the thermal loading. However, only little attention has been paid to investigate the interfacial stress transfer of carbon nanotubes with composite coatings. In the present study, the pullout models of CNTs considered as a multi-layer structure are presented to evaluate the interfacial stress transfer characteristics between the CNTs and the coatings covered on the CNTs. Moreover, the influences of the coating thickness, the wall layer numbers and the length of CNTs on the interfacial bonding characteristics are investigated and analyzed in terms of the pullout mode of CNTs.

Analytical approach

Schematic diagrams of a single CNT with coating are shown in Fig. 1. One CNT with an inner radius r_N and a outer radius r_1 is located at the center of coating materials with an outer radius b. The length of the CNT embedded within the matrix is L. The z coordinate is assigned along the symmetrical axis of the CNT, and r coordinate is the distance from the fiber axis in the radial direction. The pullout force F is the tensile loading applied to the CNT. Multi-walled carbon nanotubes (MWCNTs) can be regarded as a group of

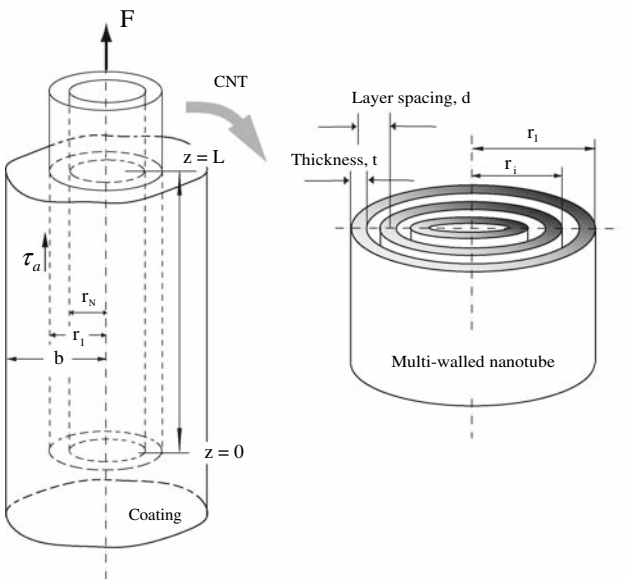

Fig. 1 Schematic diagrams of a single CNT with coating

nested single-walled carbon nanotubes (SWCNTs). Interaction between the graphene layers of MWCNT is mainly due to the van der Waals (vdW) force. Considering only small strain within the elastic limit, the interaction pressure between two adjacent nanotubes is assumed to be linear and depends on the difference of their deflections in the radial direction. Therefore, the coupled equations of the pressure caused by the vdW interaction in MWCNT layers can be given by

$$p_i = c_0(\Delta r_i - \Delta r_{i+1}) \qquad i = 1, 2, \cdots, N-1, \tag{1}$$

where Δr_i is the radial displacement in the ith layer nanotube, and p_i is vdW interaction between the ith and i + 1th CNTs. The vdW interaction c_0 can be estimated as the second derivative of the energy-interlayer spacing relation of MWCNTs. According to the data given in Girifalco and Lad [22], it is found that [23]

$$c_0 = \frac{200 erg/cm^2}{0.16 d^2} \qquad \left(d = 1.42 \times 10^{-8}\right). \tag{2}$$

The layers of CNTs can be considered as membrane shells due to the small thickness of a graphene sheet (about 0.34 nm). According to Hooke's law, the stress T_i (the force per length along circumferential direction), and the radial strain ε_i can be obtained from

$$T_i = r_i(p_{i+1} - p_i), \tag{3}$$

$$\varepsilon_i = \frac{\Delta r_i}{r_i} = \frac{T_i}{C} + v_f \frac{T_z}{C}, \qquad (i = 1, 2, \cdots, N-1) \tag{4}$$

where C is the in-plane stiffness of CNTs, and v_f is the Poisson's ratio of the CNTs. T_z is the tensile stress applied to the CNTs along the axial direction.

We assume that the ends of all shells of CNTs are well bond with the coating resin. Considering MWCNT as a group of shells packed together with uniform layer spacing d and wall thickness t, the ith layer radius of MWCNTs and the effective cross-sectional area can be expressed as

$$r_i = r_1 - (i-1)d, \tag{5}$$

$$A_{eff} = 2\pi t\left\{Nr_1 - \sum_{i=1}^{N}(i-1)d\right\}. \tag{6}$$

Substituting Eq. (1) into Eqs. (3) and (4), we obtain

$$\left(\frac{C}{r_1^2}+c_0\right)\Delta r_1 - c_0\Delta r_2 = q + \frac{v}{r_1}T_z, \tag{7}$$

$$-c_0\Delta r_1 + \left(\frac{C}{r_2^2}+2c_0\right)\Delta r_2 - c_0\Delta r_3 = \frac{v}{r_1}T_z, \tag{8}$$

$$-c_0\Delta r_{i-1} + \left(\frac{C}{r_i^2}+2c_0\right)\Delta r_i - c_0\Delta r_{i+1} = \frac{v}{r_{i-1}}T_z, \tag{9}$$

$$-c_0\Delta r_{N-1} + \left(\frac{C}{r_N^2}+c_0\right)\Delta r_N = \frac{v}{r_{N-1}}T_z, \tag{10}$$

where q is the compression pressure applied to the outer layer of MWCNT with coating due the effect of the Poisson's contraction.

Assuming that the interface between the CNTs and the coating layer are perfectly bound, a continuity condition for the radial displacement in the interface leads to

$$\frac{r_1}{E_m}\left\{\left(\frac{1+n^2}{1-n^2}+v_m\right)q + v_m\sigma_z^m\right\} + \Delta r_1 = 0,\ n = r_1/b. \tag{11}$$

where σ_z^m is the matrix stress in the axial direction. v_m and E_m are the Poisson's ratio and the elastic modulus of the coating matrix, respectively.

The solution of Eqs (7)–(11) gives the radial stress between the CNTs and the coating as

$$q = f_1 T_z + f_2\sigma_z^m \tag{12}$$

where f_1 and f_2 are functions depend on the physical properties and the geometry of CNTs and coating. In Appendix A, we give the solution of f_1 and f_2 for the double-walled CNTs.

Considering the force equilibrium conditions between the coating axial stress, CNT axial stress and interfacial stress, we have

$$\frac{dT_z}{dz} = -\tau_a, \tag{13}$$

$$\frac{d\sigma_z^m}{dz} = \frac{2r_1}{b^2-r_1^2}\tau_a, \tag{14}$$

where τ_a is the interfacial shear stress, governed by an Coulomb friction law that is proportional to the resultant radial compressive stress:

$$\tau_a = \mu(\sigma_0 + q), \tag{15}$$

where μ is the friction coefficient, and σ_0 is the residual stress from initial thermal mismatch.

Combining Eqs. (12)–(15), the differential equation of the membrane stress for CNTs yields

$$\frac{d^2T_z}{dz^2} + \mu\left(f_1 - \frac{2r_1f_2}{b^2-r_1^2}\right)\frac{dT_z}{dz} = 0, \tag{16}$$

which has the general solution:

$$T_z = A + Be^{-\gamma z}, \tag{17}$$

where

$$\gamma = \mu\left(f_1 - \frac{2r_1f_2}{b^2-r_1^2}\right), \tag{18}$$

and A and B are integral constants determined by the boundary conditions: $T_z = 0$ at $z = 0$, $T_z = T_0 = F/A_{eff}$ at z = L. Therefore, the solution of Eq (18) gives

$$T_z = \frac{T_0}{1-e^{-\gamma L}}\left(1-e^{-\gamma L}\right). \tag{19}$$

Substituting Eq. (19) into Eqs. (13) and (14), considering $\sigma_z^m = 0$ at $z = 0$, the interfacial shear stress and the coating matrix stress in the axial direction can be given by

$$\tau_a = \frac{\gamma T_0 e^{-\gamma Z}}{1-e^{-\gamma L}}, \tag{20}$$

$$\sigma_z^m = \left(\frac{2r_1}{b^2-r_1^2}\right)\frac{T_0}{1-e^{-\gamma L}}\left(1-e^{-\gamma Z}\right). \tag{21}$$

Numerical results and discussion

In the present study, the following geometric parameters for CNT and coating material properties are used

in calculations: E_{CNT} = 1 TPa, v_f = 0.27, E_m = 3.5 GPa, v_m = 0.39. A CNT has an outer radius of 2.0 nm, and a coating layer is 1.0 nm thickness. The length of embedded CNT is 200 nm. The tensile force (F) applied to the end of the CNT is 10 nN.

Figure 2 shows the distributions of the interfacial shear stress and the axial stress in the coating layer along the axial distance z/L. As shown in Fig. 2(a), the interfacial shear stress undergoes a maximum value at the pullout end of CNT. This interfacial shear stress rapidly decreases to zero as the distance from the pullout end increases. The maximum axial stress in the coating occurs at z = L (Fig. 2 (b)). This implies that the interface debonding due to the shear stress easily arises from the pullout end of CNTs, but the coating fractures in the axial direction occurs at z = L. It is seen that both maximum shear and axial stresses decrease with an increase in layer numbers of MWCNTs. The reduction of both maximum stresses can be attributed to the increased effective cross-sectional area of MWCNTs.

In the following simulation, we will only discuss the calculating results of the single-walled CNTs with composite coating. Figure 3 shows the influence of the friction coefficient on the interfacial shear stress and the axial stress in the coating. As shown in Fig. 3(a), the slope of shear stress distribution along the nanotube length increases with increasing friction coefficient between the CNT and the coating. At pullout end of CNTs, the larger friction coefficient then the larger value of maximum interfacial shear stress is. In contrast, the coating axial stress reaches the maximum value at z = L, which is independent upon the friction coefficient (Fig. 3(b)). The effects of the CNT length on the interfacial shear and the coating axial stresses are shown in Fig. 4 as the function of normalized axial position. The interfacial shear stress of CNT composites with lager nanotube length decreases rapidly away from the pullout end of CNTs (Fig. 4(a)). The maximum interfacial shear stress decreases with increasing CNT length. In the Fig. 4(b), the axial stress in the coating starts to increase at the pullout end of CNTs

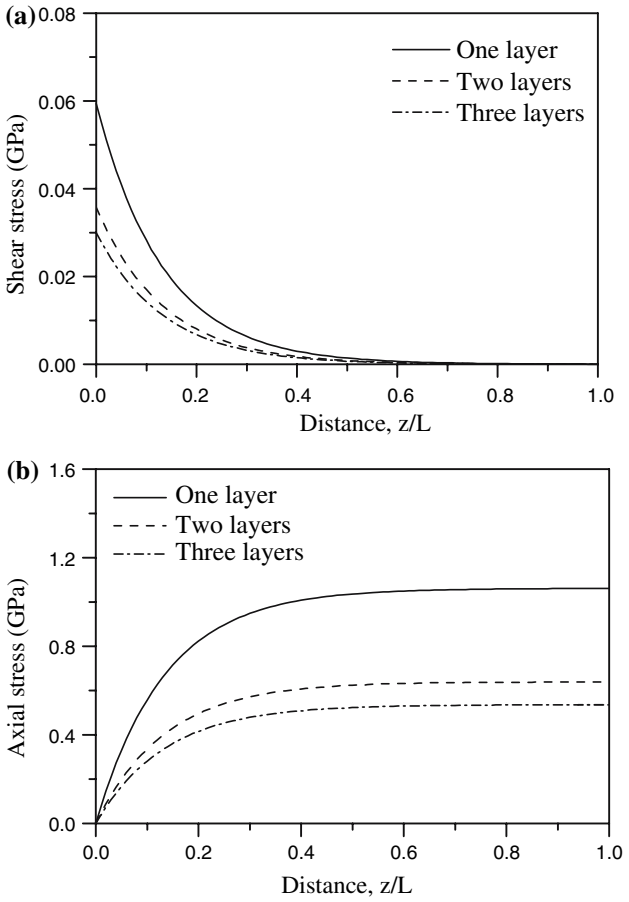

Fig. 2 Distributions of (**a**) the interfacial shear stress and (**b**) the coating axial stress along the axial distance z/L

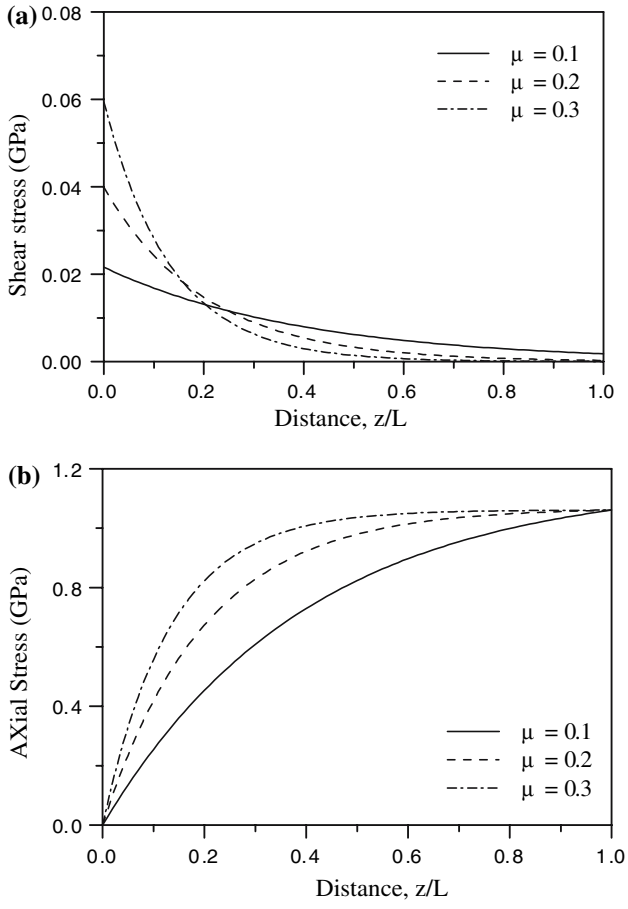

Fig. 3 Influence of the friction coefficient on the interfacial shear stress (**a**) and the coating axial stress (**b**) along the axial distance z/L

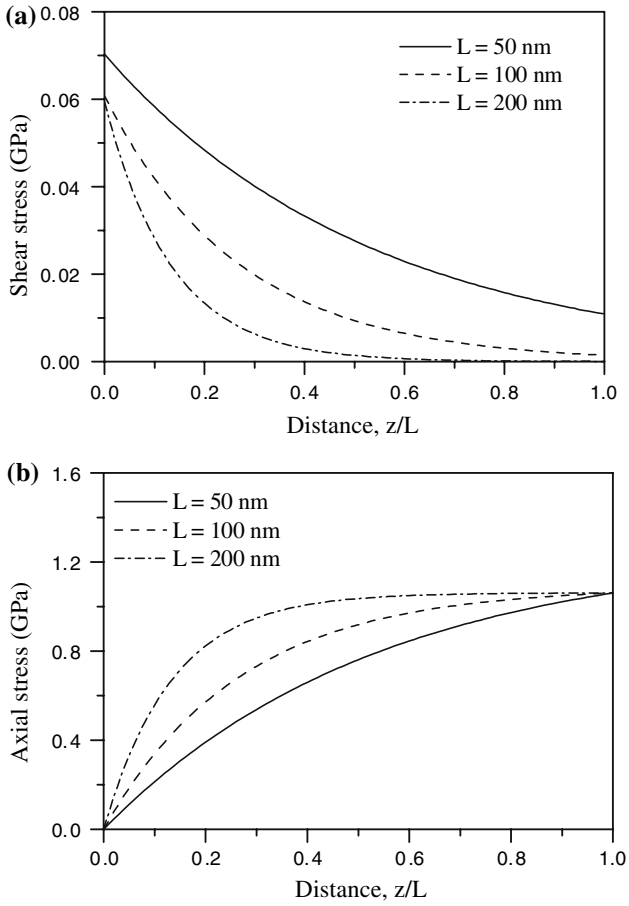

Fig. 4 Effects of the CNT length on the interfacial shear stress (**a**) and the coating axial stress (**b**) along the axial distance z/L

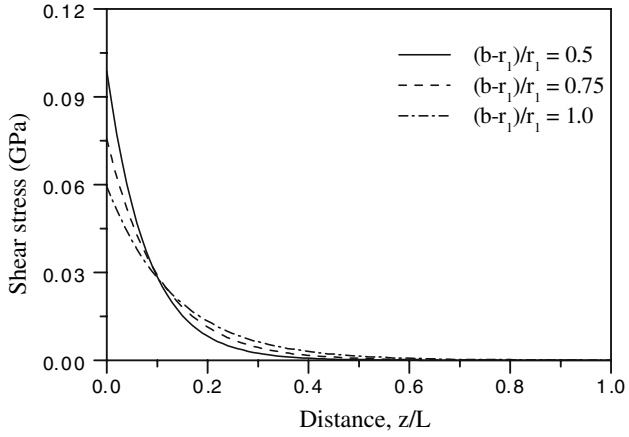

Fig. 5 Effect of coating thickness on the distribution of the interfacial shear stress as a function of CNT length

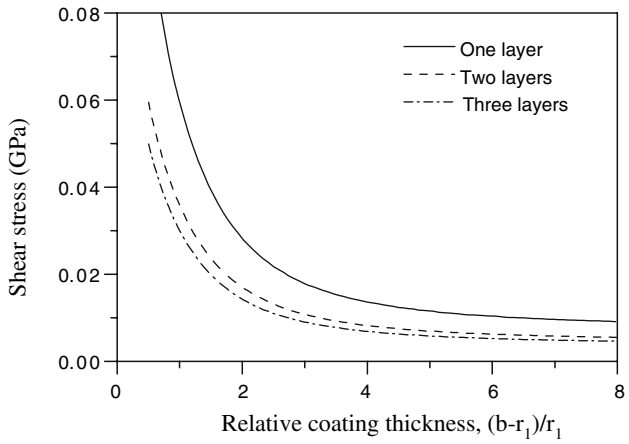

Fig. 6 Variation of the interfacial shear stress with the relative coating thickness for different layer thickness

and reaches an identical maximum value. For the aspect ratio of CNTs larger than $L/r_1 = 100$, the coating axial stress becomes to homogenously distribute over about 60% of nanotube length. Figure 5 shows the effect of coating thickness on the distribution of the interfacial shear stress as a function of CNT length. The ratios of the coating thickness to the radius of CNTs are taken as 0.5, 0.75 and 1.0. It is found that the maximum interfacial shear stress at z = 0 decreases with increasing coating thickness. As the coating is quite thin, the shear stress exhibits quite large, but reduces rapidly with increasing distance from the pullout end of CNTs. As shown in Fig. 6, furthermore, the variation of the interfacial shear stress with the relative coating thickness (coating thickness vs. CNT radius) is investigated for different layer thickness. The interfacial shear stress of the SWCNT with the coating is comparatively higher than that of MWCNT composites. The interfacial shear stress of CNT composites tends to slightly decrease down with an increase in relative coating thickness. The values of the interfacial shear stress are hardly affected by the relative coating thickness when its values is larger than 4. Figure 7 shows the ratio (η) of stress transfer from outer to inner layers when a tensile force applied to the outer shell of the CNTs. It can be found that the ratios of both axial and shear stresses tend to one. This suggests that the inner layers of the nanotubes contribute almost nothing to the stress transfer since the Van der Waals interaction between layers of CNTs is very weak. The result is in good agreement with that reported by Lau et al. [24].

Conclusions

An analytical approach has been developed to evaluate the stress transfer of CNTs with composite coatings by means of classical continuum mechanics model. The results showed that the CNT sizes, the coating

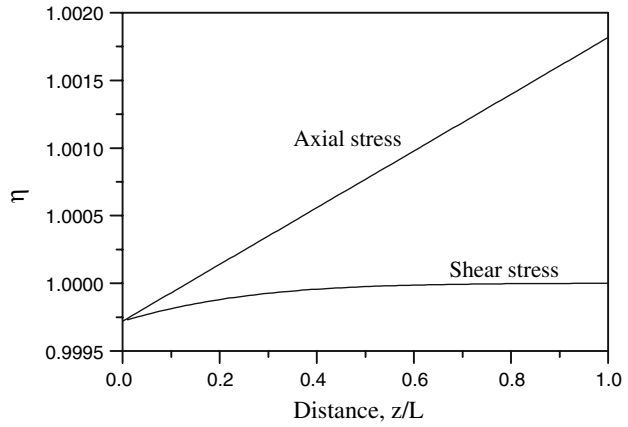

Fig. 7 Stress transfers between inner and outer layers when tensile stress applied to the outer shell of the nanotube. η: the ratio of stress defined as outer to inner layers

thickness, and the friction coefficient strongly affect the interfacial stress transforms between the CNT and the coating. The present work is a preliminary attempt for providing a theoretical calculation method to evaluate the interfacial stress transfers of CNT composites for overcoming the great difficulty in conducting their experimental investigation on a single CNT pullout test up to now. It is worthwhile mentioning that the interfacial bonding of CNT composites induced by atomic interactions with polymer chains can contributes to adhesion characteristics. The further study still needs to be done to verify the results in the present study by using the molecular dynamic (MD) method as the future extension of current work.

Acknowledgements This work was supported by the CLUSTER of Ministry of Education, Culture, Sports, Science and Technology, Japan.

Appendix A

For N = 2, the solution of Eqs (7)–(10) gives

$$\Delta r_1 = \frac{q\left(C/r_2^2 + c_0\right) + \left[\frac{v}{r_1}\left(C/r_2^2 + c_0\right) + \frac{c_0 v}{r_2}\right] T_z}{\left(C/r_1^2 + c_0\right)\left(C/r_2^2 + c_0\right) - c_0^2} \qquad \text{(A1)}$$

Substituting Eq. (A1) into Eq. (11), we have

$$f_1 = -\frac{\left[\left(C/r_2^2 + c_0\right)\frac{v_f}{\phi r_1^2} + \frac{c_0 v_f}{\phi r_1 r_2}\right]}{\left(C/r_1^2 + c_0\right)\left(C/r_2^2 + c_0\right) - c_0^2} \qquad \text{(A2)}$$

$$f_2 = -\frac{v_m}{\phi E_m} \qquad \text{(A3)}$$

and

$$\phi = \left(\frac{\left(1+n^2\right)/\left(1-n^2\right) + v_m}{E_m} + \frac{\left(C/r_2^2 + c_0\right)/r_1}{\left(C/r_1^2 + c_0\right)\left(C/r_2^2 + c_0\right) - c_0^2}\right) \qquad \text{(A3)}$$

References

1. Treacy MMJ, Ebbesen TW, Gibson JM (1996) Nature 381:678
2. Schadler LS, Giannaris SC, Ajayan PM (1998) App Phys Lett 73:3842
3. Wong EW, Sheehan PE, Lieber CM (1997) Science 277:1971
4. Vaccarini L, Goze C, Henrard L, Hernandez E, Bernier P, Rubio A (2000) Carbon 38:1681
5. Lau KT, Hui D (2002) Comp Pt B 33:263
6. Thostenson ET, Ren Z, Chou TW (2001) Comp Sci Tech 61:1899
7. Baughman RH, Zakhidov AA, de Heer WA (2002) Science 297:787
8. Chen WX, Tu JP, Wang LY, Gan HY, Xu ZD, Zhang XB (2003) Carbon 41:215
9. Chen WX, Tu JP, Gan HY, Xu ZD, Wang QG, Lee JY, Liu ZL, Zhang XB (2002) Surf Coat Tech 160:68
10. Chen WX, Tu JP, Xu ZD, Chen WL, Zhang XB, Cheng DH (2003) Mater Lett 57:1256
11. Seeger T, Redlich PH (2001) Chem Phys Lett 339:41
12. Han WQ, Zettl A (2004) Nano Lett 3:681
13. Zhao L, Gao L (2004) Carbon 42:1858
14. Shi D, Lian J, He P, Wang LM, Ooij WJv, Schulz M, Mast DB (2002) App Phys Lett 81:5216
15. Shi D, Lian J, He P, Wang LM, Xia F, Yang L, Schulz MJ, Mast DB (2003) App Phys Lett 83:5301
16. Patil A, Sippel J, Martin GW, Rinzler AG (2004) Nano Lett 4:304
17. Hsueh CH (1988) J Mater Sci Lett 7:497
18. Lau KT (2003) Chem Phys Lett 370:399
19. Zhang YC, Wang X (2005) Inter J Solid Stru 42:5399
20. Timoshenko SP, Goodier JN (1951) Theory of elasticity. McGraw-Hill, New York
21. Xiao KQ, Zhang LC (2004) J Mater Sci 39:4481
22. Girifalco LA, Lad RA (1956) J Chem Phys 25:693
23. Ru CQ (2000) Phys Rev B 62:16962
24. Lau KT, Gu C, Gao GH, Ling HY, Reid SR (2004) Carbon 42:423